FTIR Microspectroscopic Study of Cell Types and Potential Confounding Variables in Screening for Cervical Malignancies

BAYDEN R. WOOD,[1] MICHAEL A. QUINN,[2] BRIAN TAIT,[3] MARTIN ASHDOWN,[4] TRACY HISLOP,[1] MELISSA ROMEO,[1] DON McNAUGHTON[1]

[1] Department of Chemistry, Monash University, Wellington Road, Clayton, Victoria 3168, Australia

[2] Department of Obstetrics and Gynaecology, University of Melbourne, Grattan Street, Parkville, Victoria 3052, Australia

[3] Department of Tissue Typing, Royal Melbourne Hospital, Grattan Street, Parkville, Victoria 3052, Australia

[4] 140 Keon Street, Thornbury, Victoria 3071, Australia

Received 5 June 1997; revised 18 June 1997; accepted 1 October 1997

ABSTRACT: FTIR microscopy was applied to the analysis of cell types and other variables present in Pap smears to ascertain the limitations of infrared spectroscopy in the diagnosis of cervical cancer and dysplasia. It was found that leukocytes, and in particular lymphocytes, have spectral features in the phophodiester region (1300–900 cm^{-1}) suggestive of what has previously been described as changes indicative of malignancy. Endocervical cells and fibroblasts have similar spectral features to HeLa cells and consequently could also confound diagnosis. The use of ethanol as a fixative and dehydrating agent results in retention of glycogen in cervical cell types and thus minimizes spectral changes in the glycogen region due to sampling technique. Spectra of seminal fluids exhibit strong bands in the phosphodiester/carbohydrate region; however, sperm contamination should be easily detectable by the presence of a distinctive doublet at 981/968 cm^{-1}. Erythrocyte spectra exhibit a reduction in glycogen band intensity, but can be discerned by a relatively low-intensity $\nu_s\ PO_2^-$ band. Endocervical mucin spectra exhibit a reduction in glycogen bands and a very pronounced $\nu_s\ PO_2^-$ band, which is similar in intensity to the corresponding band in HeLa cells. Thrombocytes have strong bands in the phosphodiester region, but thrombocytes can be discerned from other cell types by the presence of two small broad bands at 980 and 935 cm^{-1}. *Candida albicans* is characterized by strong bands in the polysaccharide region which could potentially obscure diagnostic bands if *C. albicans* is present in large numbers. Spectra of bacteria common to the female genital tract, in general, also have strong absorptions in the polysaccharide region; however, bacterial contamination is usually minimal and would not be expected to obscure cervical cell spectra. Nylon threads and bristles from cervical sampling implements produce characteristic IR profiles which allow for easy identification. Given the number of potential confounding variables associated with cervical cytology, a multivariate statistical or neural network analysis would appear to be necessary before the implementation of FTIR technology in clinical laboratories. © 1998 John Wiley & Sons, Inc. Biospectroscopy 4: 75–91, 1998

Keywords: FTIR microspectroscopy; cervical cancer; leukocytes; lymphocytes; erythrocytes; semen; mucins; fibroblasts; thrombocytes; bacteria; nylon; *Candida albicans*

Correspondence to: D. McNaughton (d.mcnaughton@sci.monash.edu.au).

Contract grant sponsors: Royal Women's Hospital; Australian Research Council.

Biospectroscopy, Vol. 4, 75–91 (1998)
 CCC 1075-4261/98/020075-17

INTRODUCTION

For some time alternative techniques for the detection of dysplastic and malignant cell and tissue samples have been under investigation, with the aim of reducing the current reliance on the more subjective traditional diagnostic methods which are prone to human error or misdiagnosis. Many spectroscopic methods have been examined in this context,[1–19] and infrared and Raman spectroscopy in particular show much promise.[5–19] A number of recent studies[13–19] have investigated the potential of Fourier transform infrared (FTIR) spectroscopy as a diagnostic tool for the early detection of cervical cancer, and all show that biochemical changes associated with the diseased state can be detected. These changes can be attributed to the macromolecular changes associated with the transformation from normal to dysplastic (precancerous) and malignant cell types.

In our previous study[16] spectra of cervical samples containing a mixture of endo- and ectocervical cells were analyzed using principal component analysis (PCA). The results of that study indicated that PCA could be used to discriminate normal from abnormal cell types on a two-dimensional (PC1 vs. PC2) scores plot. The best discrimination was obtained when the data was reduced to seven specific wavenumber values distributed over the 1600–1000 cm^{-1} region. While a large percentage of smears could be correctly grouped, the separation was not totally distinct, as some small overlap of normal and abnormal diagnosed samples was observed. We are continuing to pursue this multivariate statistical approach by building a larger data set and extending the study into the use of artificial neural networks. Although the results of the PCA study and the previous studies of others are promising, further work is required to identify and if possible eliminate those variables and contaminants that may confound spectroscopic diagnosis. This work is concerned with the identification of the cell types and variables that may confound diagnosis, with the aim of improving the sensitivity and specificity of this diagnostic technique.

The cytology of smears sampled from the cervix is complex. A variety of cell types including endocervical cells, squamous ectocervical cells, erythrocytes, leukocytes, and platelets (thrombocytes) can be collected in a routine smear of a healthy patient. Samples may also contain a plethora of bacteria, yeast, semen, and other contaminants including synthetic threads and bristles from the cervical sampling implements. In patients with abnormalities due to disease, the variety of cells is increased further with a proliferation and localized accumulation of leukocytes (namely lymphocytes, monocytes, and polymorphs) as a result of the immune response. In some invasive cancers an increase in connective tissue, which can contain collagen fibers, macrophages, and fibroblasts is apparent. In this work we have isolated the majority of these cells and contaminants and recorded their infrared spectra. These spectra are compared with the spectra of cervical samples diagnosed as normal by the Victorian Cytology Service (VCS) and that of HeLa cells, a cultured strain of malignant cervical cells which will serve as a benchmark for comparison in this study. The aim of this study is to elucidate which cells or contaminants are likely to confound or complicate any diagnostic technique based on FTIR spectroscopy.

EXPERIMENTAL

Spectroscopic Methods

FTIR analysis was performed with a Perkin–Elmer microscope fitted with a liquid nitrogen cooled mercury–cadmium–telluride (MCT) detector coupled to a Perkin–Elmer 1600 spectrometer. Spectra were recorded in the midinfrared from 4000 to 750 cm^{-1}. The majority of spectra were taken by depositing a suspension of cells into a purpose-built multicavity IR cell, the details of which have been previously described.[16] The cell consists of a KRS-5 crystal ($50 \times 30 \times 5$ mm) clamped between two aluminum plates. The top plate has 15 regularly spaced 5-mm-diameter cavities, each countersunk to allow the positioning of O-rings. After evaporation of the solvent (by vacuum desiccation) a thin circular deposit of cells is available to record spectra. For each sample a minimum of six or eight spectra were recorded over the deposited cells in order to assess reproducibility. Each spectrum consisted of 16 coadded scans at a resolution of 8 cm^{-1}. The spectra were transferred in JCAMP–DX format to an IBM compatible computer and processed using OPUS/IR version 2.0 software. The spectra were first baseline corrected using the "rubber band" algorithm with 20 baseline points selected and then normalized using an "interactive Min/Max" normalization centered on the amide I region

(1700–1630 cm^{-1}). Unless otherwise stated, the individually recorded spectra of each sample were consistent, and the spectra presented in this article are averages of the six or eight spectra recorded for each sample contained in the single multicavity IR sample well. The spectra of extracted blood components (leukocytes and erythrocytes) presented, unless otherwise stated, were the averaged profiles from six volunteers.

Sample Preparation

Cell Types

Ectocervical and Endocervical Cells. Cervical samples from 62 patients were collected at the Royal Women's Hospital Dysplasia Clinic (Melbourne, Australia). The samples were taken from the transformation zone of the cervix and included ectocervical cells which were collected with an Ayre spatula, and endocervical cells which were sampled with a Cytobrush™. Each implement was placed in a separate 50-cm^3 centrifuge tube containing between 10 to 20 cm^3 of ethanol.

A small portion of each sample was retained for Pap smear analysis by the VCS. For Pap smears classified as abnormal or inconclusive by the VCS, follow-up biopsies were ordered, and the results made available to the authors after the infrared spectra were analyzed. Of the 29 patients diagnosed by biopsy, 7 were diagnosed cervical intraepithelial neoplasia class III (CINIII); 12 were diagnosed CINII; and 10 were diagnosed human papilloma virus (HPV)/CINI. The 33 remaining samples were diagnosed normal by Pap smear with no follow-up biopsy ordered. Endocervical cells were also collected from a hysterectomy specimen by slitting open the cervix and sampling with a Cytobrush directly. This method ensures that no ectocervical cells will be present in the sample. The portion for infrared analysis was deposited by agitating the cervical sampling implements in absolute ethanol in 50-cm^3 centrifuge tubes. The sample was centrifuged (3000 g for 5 min), and the excess ethanol removed. The cellular material was then suspended in the remaining ethanol with the aid of a vortex mixer and transferred by a Gilson Pipetteman™ into the multicavity IR cell. The infrared cell, its cavities loaded with cellular suspensions, was placed in a vacuum desiccator and the ethanol removed by evaporation to leave the samples as thin even discs of cervical cells on the crystal. For each sample six spectra were recorded for both ectocervical and endocervical cells.

HeLa Cells and Malignant Cells. HeLa cells, a cultured malignant cervical cell line, were prepared as previously described.[16] Malignant cells from a patient with carcinoma *in situ* were collected from a hysterectomy specimen by slitting open the cervix and sampling with a Cytobrush directly and treated in the same way as above.

Extraction of Blood Components

Fifty cubic centimeter blood samples were obtained from six volunteers at the Monash University Health Service (Melbourne).

Extraction of Erythrocytes and Leukocytes

Ten cubic centimeter aliquots of blood were placed in lithium coated anticoagulant tubes and then transferred to narrow 5-cm^3 centrifuge tubes and centrifuged at 2700 rpm for 15 min. In this process the erythrocytes form a pellet at the bottom of the tube, while the majority of leukocytes form a thin layer at the interface between the erythrocyte and plasma layers. The leukocyte and erythrocyte fractions were carefully removed in separate Pasteur pipettes, washed six times in 0.9% saline to remove the majority of thrombocytes, and deposited into the cavities of the multicavity IR cell.

Lymphocyte and Thrombocyte Extraction

Fifteen cubic centimeters of each blood sample was collected in Na/heparin anticoagulant coated tubes. Each individual sample of blood was then transferred to 50-cm^3 centrifuge tubes and diluted with an equal volume of 0.9% saline solution. Twenty cubic centimeters of Lymphoprep™ (Nycomed Pharma AS Prod. No. 221395) was carefully layered underneath the diluted blood and the whole sample centrifuged at 2300 rpm for 15 min. After centrifugation, the majority of mononuclear cells were removed from the interface of the lower lymphoprep layer and the upper plasma layer (which contains mainly thrombocytes) using a Pasteur pipette. The harvested fraction containing mainly lymphocytes was transferred to a 10-cm^3 centrifuge tube and diluted in 0.9% saline to reduce the density of the solution. The suspension was centrifuged at 3200 rpm for 5 min to pellet the lymphocytes, which were then resuspended in 0.9% saline and centrifuged at 2700

rpm for a further minute. The majority of mononuclear cells form a pellet at the base of the tube while the majority of thrombocytes remained in the supernatant. This final washing and thrombocyte extraction process was repeated three times before the pelleted lymphocytes were agitated and then placed into the IR cell cavity. Thrombocytes were harvested from the original supernatant in the above protocol. This was achieved by suspending the thrombocytes in 0.9% saline and then transferring them using a plastic sterile pipette to a 1.5-cm^3 Eppendorph tube. The tube was centrifuged for 15 min at 3000 rpm and the resulting pellet then resuspended in 100 μL of saline and transferred by Pasteur pipette to the multicavity IR cell for analysis.

Fibroblasts

Fibroblasts were first obtained in small numbers by transcervical chorionic villus sampling and then cultured over a long term to provide a large enough sample for analysis. Transcervical chorionic villus sampling involved passing a cannula through the vagina and the cervix, into the uterus and finally into the developing placental tissue (chorionic villis). Suction was then applied to a syringe at the end of the cannula and ca. 20 mg chorionic villi was aspirated into the syringe and placed into phosphate-buffered saline (PBS). The villi were dissected, the PBS removed, and 3 drops of 0.25% trypsin in Hanks Balanced Salt Solution with antibiotics (ICN/Flow Cat. No. 18-894-54) were added. The villi was then finely minced with a No. 22 scalpel blade and scraped into a petri dish. Trypsin (1 cm^3) was added with a sterile plastic pipette to the macerated villi, the mixture was then aspirated, transferred to a sterile centrifuge tube, agitated, and then incubated at 37°C for 90 min.

After incubation the tube was agitated to resuspend the villi and 5 cm^3 of Medium 199 supplemented with 20% fetal bovine serum was added. This medium was used to wash the villi and neutralize the trypsin. After centrifugation for 5 min at 1800 rpm, the supernatant was removed and the pellet resuspended in 2.5 cm^3 of AminoMax medium (Gibco BRL Prod. No. 17001-017) and then placed in a 12.5-cm^3 flask. One drop of penicillin/streptomycin/fungizone solution was added as a precaution and the culture incubated at 37°C for 3 weeks with $\approx$ 5% CO_2 (Oxoid Gas Generating Kit Anaerobic System, Code No. BR38, mixed in a 3.5-L gas jar). The fibroblasts were then washed in PBS and removed from the side of the flask by the addition of 1 cm^3 of trypsin. The resultant suspension was transferred to a 1.5-cm^3 Eppendorf tube, centrifuged at 2900 rpm for 5 min, and then washed three times in 0.9% isotonic saline. The cells were resuspended in 100 μL of saline and transferred to the multicavity IR cell, rapidly desiccated under vacuum, and then analyzed with the FTIR microscope.

Preparation of Microorganisms

The microorganisms examined in this study are listed in Table I together with the specific culture media, incubation times, and growth conditions (anaerobic or aerobic). Each strain was streaked onto agar using the four-quadrant streak pattern.[20] For the transfer of the cultured microorganisms a swab was first moistened in 0.9% isotonic saline and the microbes carefully removed to avoid media contamination. The microbes were suspended in 2 cm^3 of 0.9% isotonic saline, contained within a 10-cm^3 centrifuge tube, and stored at 4°C before transference to the multicavity infrared cell. To ensure the spectra obtained were reproducible the microbes were cultured a second time and the experiment repeated.

Semen Analysis

Ejaculant from two volunteers was used in this analysis. Each volunteer smeared a portion of the sample evenly onto a KRS-5 disc. The disc was desiccated under vacuum and then analyzed with the FTIR microscope.

Mucins

Mucosubstances from a volunteer were collected during the secretory phase of the menstrual cycle with a vaginal swab and smeared evenly onto a KRS-5 substrate.

Unidentified Threadlike Objects (UTLOs)

The FTIR microscope facility is equipped with a knife-edge aperture enabling the researcher to encapsulate a particular region of interest and then record an IR spectrum. This feature was used to investigate UTLOs that could not be classified by morphology. For each UTLO two spectra were re-

Table I. Growth Culture Conditions and Range of Incidence of Microorganism in Female Genital Tract

Species	Range of Incidence (%)[a]	Culture Medium	Conditions	Incubation Time
Staphylococcus aureus	5–15	Nutrient agar	O_2	22 h
Staphylococcus epidermidis	35–85	Horse blood agar	O_2	22 h
Enterococcus faecalis	30–80	Horse blood agar	O_2	22 h
Streptococcus pyogenes	5–20	Horse blood agar	O_2	22 h
Lactobacillus acidophilus	50–75	Horse blood agar	O_2	48 h
Corynebacterium hofmanni	45–75	Horse blood agar	O_2	22 h
Clostridium perfringens	15–30	Horse blood agar	AnO_2	22 h
Bacteroides fragilis	60–80	Horse blood agar	AnO_2	22 h
Acinetobacter anitratus	5–15	Nutrient agar	O_2	22 h
Gardnerilla vaginalis	5–10	Horse blood agar	O_2	22 h
Candida albicans	30–50	Malt agar	O_2	48 h

AnO_2, grown under anaerobic conditions in an anaerobic gas jar; O_2, grown under aerobic conditions.
[a] Range of incidence refers to the percentage of women infected by the microorganism from *Techniques Manual,* Department of Microbiology, University of Melbourne, February 1995.

corded and compared with a polymer data bank generated in our laboratories.

Bristles From Sampling Implements

Bristles from the Cytobrush were removed from the brush with a scalpel and placed onto a KRS-5 crystal. The bristles were individually targeted with the knife-edge aperture and the spectra recorded.

RESULTS AND DISCUSSION

HeLa and Malignant Cell Types

The spectra of the HeLa cells were, by simple visual examination, essentially the same as those of the carcinoma *in situ* samples. HeLa cell spectra are thus used in the following discussion as the basis for spectral comparison.

Endocervical and Ectocervical Cell Types

For the spectra of the 29 abnormal samples considerable variation was found in the 8 ectocervical spectra recorded over each sample, whereas for the 33 normal samples the 8 ectocervical spectra were essentially the same by visual examination. For the endocervical cells, a visual comparison of all spectra determined no obvious differences between normal and abnormal cell types.

A Pap smear is deemed representative of the transformation zone of the cervix, where the onset of cancer occurs, if both endocervical and ectocervical cells are present in the smear. This part of the present study was undertaken to obtain spectra of separate samples of endo- and ectocervical cells in order to determine whether infrared spectroscopy could be used to distinguish between the two cell types. Figure 1 depicts the averaged spectra of ectocervical and endocervical cells from 33 patients diagnosed as normal by Pap smear and the averaged spectra of the HeLa cells. The averaged spectra are presented because the individual spectra were superimposable. The spectra of endocervical cells from the hysterectomy sample were almost identical to the spectra of endocervical cells collected from above the transformation zone of the cervix by the Cytobrush, indicating that ectocervical cell contamination was minimal as a result of transformation zone sampling.

The following assignments are made based on previous FTIR studies[13–19,21–31] on whole cells, organelles, and macromolecules.

It can be seen on visual inspection, that the spectrum of endocervical cells is different to that of ectocervical cells and more closely resembles the spectrum of HeLa cells, particularly in the phosphodiester region (between 1200 cm^{-1} and 950 cm^{-1}). Endocervical cells, like HeLa cells, exhibit reductions in peak intensities at 1024 cm^{-1} and 1050 cm^{-1}. These bands are normally associated with C—O stretches of carbohydrate moieties.[14,21,31] The spectra also show pronounced

bands due to ν_s PO_2^- and ν_{as} PO_2^- at 1080 cm^{-1} and 1240 cm^{-1} respectively, as a consequence of the high nuclear-to-cytoplasmic ratio in endocervical cells.[18] Wong et al.[18] independently observed a reduction in glycogen band intensity and very pronounced phosphate bands and concluded that samples containing a large number of endocervical cells could confound spectral diagnosis. The spectra recorded in this study show slight differences to those recorded by Wong et al., in particular, we noted a reversal in the relative intensities of the ν_s PO_2^- at 1080 cm^{-1} and the C—O stretch at 1024 cm^{-1} associated with glycogen. This is most likely due to differences in the sample preparation. Wong et al. initially deposited the cervical cells in saline solution whereas we used absolute ethanol. Once cells are removed from the *in vivo* state ischemic damage occurs and the autolytic process begins. This results in cellular constituents (including glycogen) being broken down. Hopwood[32a] states that in aqueous physiological solutions glycogen loss can be as high as 60–80% and that alcohol-based fixatives are recommended for glycogen fixation. This is because glycogen breaks down into glucose monomers which leach out of the cells into the surrounding solution. Ethanol, on the other hand, is a coagulative protein fixative and dehydrating agent. There are two main theories regarding glycogen fixation. One hypothesis suggests that glycogen is fixed by ethanol through the removal of surrounding water molecules. The second and more widely held view is that glycogen preservation is achieved through fixation of associated proteins.[32b] This, in combination with the fact that glycogen is insoluble in ethanol, results in the stabilization and localization of glycogen within the cell, that is, preventing glycogen from leaching out. On the other hand, ethanol can cause protein aggregation of some but not all proteins; however, it does not denature nuclear proteins.

The spectral features of normal ectocervical cells are similar to those classified by Wong et al. as indicative of normal epithelial tissue and cells.[13,14,18] The similarities include (1) bands at 1650 cm^{-1} and 1541 cm^{-1} that arise from the amide I (predominantly the C=O stretching vibration of the amide), and amide II absorption (primarily an N—H bending coupled to a C—N stretching vibrational mode) of tissue proteins, respectively;[29] (2) a band at 1454 cm^{-1}, which is attributed to the asymmetric methyl deformation mode found ubiquitously in biomolecules;[18] (3) a band appearing at 1400 cm^{-1} from the symmetric stretch of methyl groups in proteins;[18] (4) an intense C—O stretching vibration at 1155 cm^{-1}; (5) an asymmetric phosphate stretching (ν_{as} PO_2^-) band at 1244 cm^{-1} and a pronounced symmetric phosphate stretching (ν_s P_{O2}^-) band at 1078 cm^{-1}; (6) intense glycogen bands at 1050 and 1022 cm^{-1}; (7) previously unreported by Wong et al. is a small band at 938 cm^{-1} which is unassigned.

With the marked differences between normal endo- and ectocervical cells it should be possible, at least in the case of normal smears, to determine whether a particular cervical sample is indeed representative of the transformation zone.

Considerable differences exist between spectra of normal ectocervical cells and HeLa cells. In the HeLa profile, the glycogen bands have almost disappeared and a band at 1037 cm^{-1} has emerged. The ν_s PO_2^- band (now at 1079 cm^{-1}) is pronounced, and is of similar intensity to the ν_{as} PO_2^- band appearing at 1246 cm^{-1}. This is in contrast to the normal ectocervical profile, where the ν_s PO_2^- peak appears to be significantly more intense than the ν_{as} PO_2^- peak, because the ν_s PO_2^- peak is overlapped by the intense glycogen band. HeLa cell spectra are also characterized by an increase in the intensity of the amide II band relative to the amide I band. This increase in the amide II band is also the case in all the spectra of the smear samples categorized as abnormal by cytology. The PCA loadings plot shown in our previous work also indicates this region is important in the separation of normal and abnormal categories.[16]

To determine which of the two cell types (ectocervical and endocervical) is more applicable to IR analysis we applied PCA to ectocervical and endocervical samples and found that the ectocervical samples form far tighter clusters and give a far better separation for normal and abnormal diagnosed samples compared to spectra from endocervical samples. The better separation is possibly the result of greater molecular disparity between normal ectocervical samples and abnormal cytologically diagnosed samples. Alternatively, the better separation may be related to the fact that cervical lesions are predominantly of the squamous cell variety. The results of this PCA analysis will be presented elsewhere.

Potential Confounding Variables

Table II contains a list of potential confounding variables commonly found in cervical samples to-

gether with a classification. Spectra of these variables are classified by visual inspection by comparison with bands in the phosphodiester region considered in previous work as being useful for diagnosis.[13,14,19,24] These classifications are confounding, nonconfounding, or unique (the spectral fingerprint may overlap the phosphodiester region; however, the contaminant can be easily identified from characteristic peaks).

Blood Components

Leukocytes

Leukocytes can be divided into two main groups: granular, which include basophils, neutrophils, and eosinophils; and nongranular, which include lymphocytes and monocytes. The relative proportions of these cell types in blood are neutrophils, 55–60%; eosinophils, 1 to 3%; basophils, 0 to 0.7%; lymphocytes, 25–33%; monocytes, 3–7%.[33] Different disease processes and tissue damage may cause a proliferation of specific cell types. Figure 2 depicts six spectra recorded of leukocytes extracted from a blood sample from one of the volunteers. Due to the variation in the proportions of different cell types the spectra recorded over the sample well exhibited some variation. However, in general the spectra of leukocytes exhibit features suggestive of malignant transformation of the cervical epithelium when only the phosphodiester region is considered. Most notably they show a reduction in glycogen band intensity at 1024 cm^{-1} and 1050 cm^{-1} and pronounced symmetric and asymmetric phosphate stretches at 1078 cm^{-1} and 1240 cm^{-1}, respectively.

In order to provide more insight into which leukocyte components exhibit spectral features in the phosphodiester region, a lymphocyte extraction was performed on fresh blood. Lymphocytes can be classified into two major lineages: T-cells (thymus-derived) and B-cells (bone-marrow-derived). The relative proportions of these two major lineages in peripheral blood are 75 and 10%, with the remaining 15% of peripheral blood lymphocytes belonging to the lineage known as the natural killer cells.[34] While lymphocytes are commonly detected in most Pap smears their numbers are usually small. Lymphocyte numbers can become significant when there is an underlying pathological

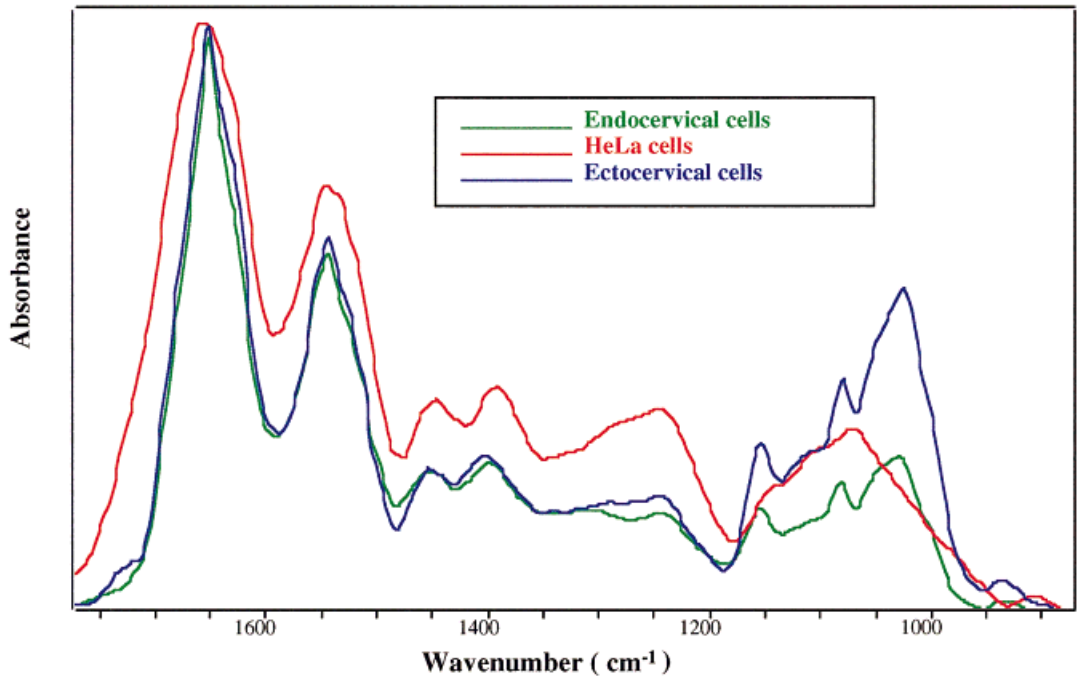

Figure 1. Infrared spectra of normal ectocervical cells, normal endocervical cells, and HeLa cells.

Table II. Classification of Common Components of Pap Smears

Common Pap Smear Component	Possibly Confounding	Nonconfounding	Unique
Endocervical cells	X		
Leukocytes			
Granulocytes	X		
Lymphocytes	X		
Erythrocytes		X	
Thrombocytes			X
Fibroblasts	X		
Bacteria			
Staphylococcus aureus		X	
Staphylococcus epidermidis		X	
Enterococcus faecalis		X	
Streptococcus pyogenes		X	
Lactobacillus acidophilus		X	
Corynebacterium hofmanni		X	
Clostridium perfringens		X	
Bacteroides fragilis		X	
Acinetobacter anitratus		X	
Gardnerilla vaginalis		X	
Yeast			
Candida albicans	X (Only in a small % of smears)		
Mucins	X		X
Semen	X		X

process such as infection, a cervical lesion, or other lesions of the uterus. The spectra of lymphocytes, shown in Figure 3, exhibit much less variability over the sample well when compared to the leukocyte spectra, due to the reduced number of differing cell types. The spectra show a reduction in glycogen band intensity in the 1050–1020 cm^{-1} region similar to leukocyte spectra but with a very intense ν_s PO_2^- at 1080 cm^{-1} and a more pronounced ν_s PO_2^- at 1240 cm^{-1}. Consequently, the potential for erroneous diagnoses is increased if the transformation zone of the cervix or surrounding tissue is inflamed, and visual inspection of the phosphodiester region is considered as the only diagnostic region.

Erythrocytes

Unlike leukocytes, erythrocytes are frequently observed in smears, and can be found in large numbers in a small percentage of smears. The presence of erythrocytes results from (1) cervical sampling during the flow phase of the menstrual cycle, (2) tissue damage as a result of the sampling procedure, or (3) cervical lesions where bleeding is symptomatic. Erythrocyte spectra exhibit a reduction in glycogen band intensity (a characteristic of HeLa cells); however, the spectra can be readily discerned from abnormal samples by examination of their distinctive phosphate peaks. Erythrocyte spectra exhibit only diminutive phosphate peaks, due to the deficiency in nucleic acids, and so can be spectroscopically discerned from other cell types encountered. Erythrocytes can also be readily distinguished from lymphocytes and thrombocytes by examination of the phosphodiester region (1300–900 cm^{-1}). Figure 4 compares the phosphodiester region of erythrocytes, lymphocytes, and thrombocytes. It is apparent that the ν_s PO_2^- at 1080 cm^{-1} in the erythrocyte spectra is dramatically reduced compared to the other spectra.

Thrombocytes

Thrombocytes are often observed in Pap smear samples. Their numbers can become significant

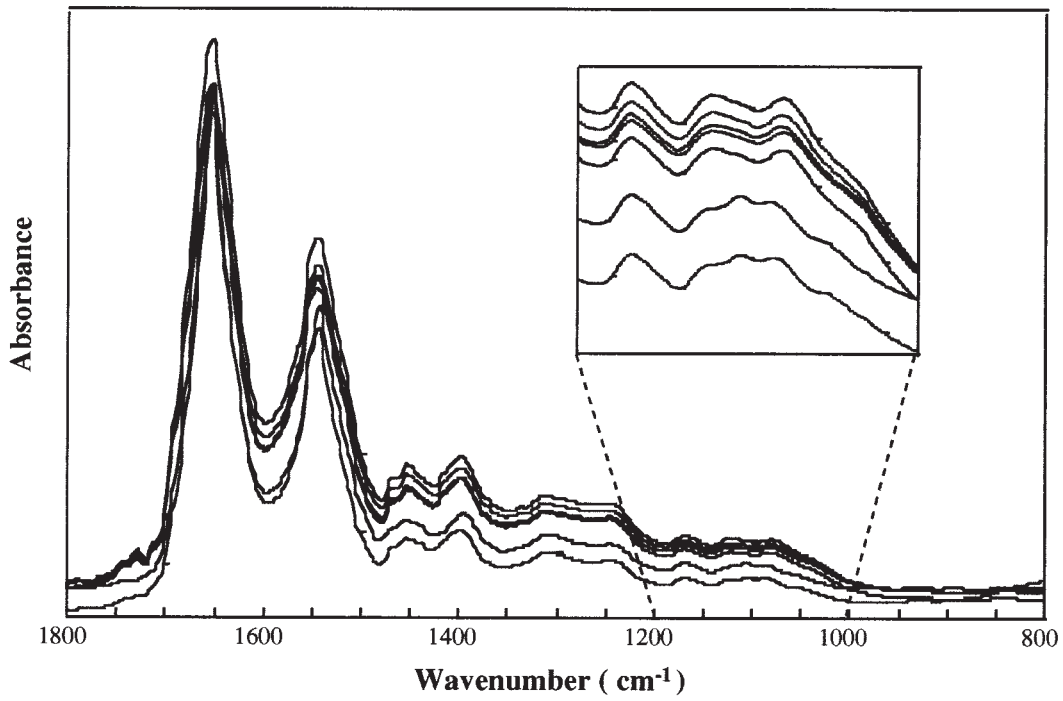

Figure 2. Infrared spectra of leukocytes from one volunteer showing variation over the 8 recorded spectra. The insert depicts the expanded view of the phosphodiester region 1200–1000 cm^{-1}.

as a consequence of a cervical lesion or tissue damage where thrombocyte aggregation arises as part of the initial clotting mechanism. Thrombocyte spectra are characterized by intense ν_s PO_2^- and ν_{as} PO_2^- bands at 1080 cm^{-1} and 1240 cm^{-1} possibly due to a combination of phosphorylated proteins such as adenosine diphosphate (ADP) found in thrombocyte granules and phospholipid cofactors which, like ADP, are secreted to facilitate thrombocyte aggregation.[35] However, thrombocyte spectra can be discerned from other cell types by examination of the region below 1000 cm^{-1}. Thrombocyte spectra exhibit two small broad characteristic bands at 980 cm^{-1} and 935 cm^{-1} which are presently unassigned (Fig. 4).

Connective Tissue

Fibroblasts

In general, fibroblasts and connective tissue are rarely sighted in normal cervical smears; however, they may be observed in severe cases of carcinoma *in situ* and invasive carcinoma. Spectra of fibroblasts, shown in Figure 5, exhibit spectral features similar to HeLa cells, with strong bands appearing at 1240 cm^{-1} and 1080 cm^{-1} which may arise from overlapping collagen and phosphate bands.[23] Jackson et al.[23] noted the possibility of incorrect band assignment for cancerous cells surrounded by a connective tissue matrix as is the case in breast tumors. They demonstrated that collagen bands associated with connective tissue could be misassigned as DNA absorptions. However, in the case of the cervix, the detection of connective tissue could be diagnostic for severe invasive carcinoma, as the composition of the cervical transformation zone is predominantly squamous and columnar cells.

Other Potential Confounding Variables

Seminal Plasma

Spectra of semen from normal sperm-producing males are shown in Figure 6 and exhibit strong peaks in the phosphodiester region (1200–1000 cm^{-1}) that could confound spectroscopic diagnosis if this region alone is used. However, the spectra also exhibit a number of characteristic features that enable sperm contamination to be identified in cervical samples. The most striking features

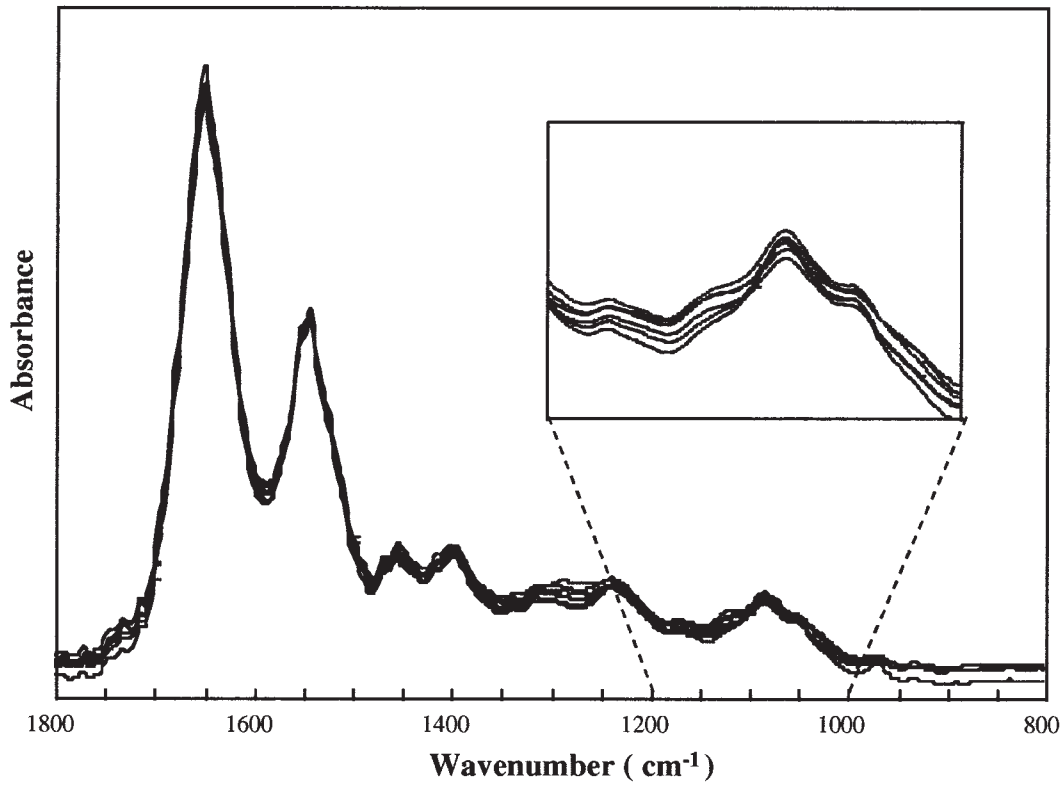

Figure 3. Six recorded spectra of lymphocytes from one volunteer. The spectra exhibit much less variation over the region than do leukocyte spectra. The insert depicts the expanded view of the phosphodiester region 1200–1000 cm^{-1}.

include (1) an intense amide II band at approximately 1550 cm^{-1}, (2) a prominent band at 1400 cm^{-1} normally associated with the COO^- group of fatty acids and amino acids,[13] (3) a very intense broad band at 1084 cm^{-1}, and (4) a most distinctive doublet appearing at 981 and 968 cm^{-1} which at present is unassigned.

Nylon Threads

Cervical smears often contain a variety of threads which may result from clothing debris or alternatively from tampons. Figure 7 shows the spectrum of an example of a threadlike object embedded in cervical tissue that was spectroscopically identified as that of nylon. Spectra of nylon threads display bands that overlap the diagnostic region (1600–950 cm^{-1}) of cervical cells; however, nylon is easily identified by a number of characteristic bands. The most prominent features are the N—H stretching band at 3300 cm^{-1}; the carbonyl at 1650 cm^{-1}; and other characteristic nylon vibrations at 3081, 1546, 1463, 1418, 1265, 1200, 1171, and 930 cm^{-1}.

Cervical Sampling Implements

Bristles from the Cytobrush, if present, could also interfere with spectroscopic diagnosis, although spectra taken by us show they can be easily discerned by a number of characteristic bands. To date we have not observed these bristles in any of the spectra taken of cervical smears.

Microorganisms

Bacteria

Figure 8 shows spectra from 5 of the 12 microbes investigated. Significant differences exist between the various strains enabling taxonomic discernment as reported by Nauman et al.[36–39] The spectra of the common cervical bacteria we investigated, in general, exhibit a strong asymmetric phosphate band at 1245 cm^{-1}, and a very intense

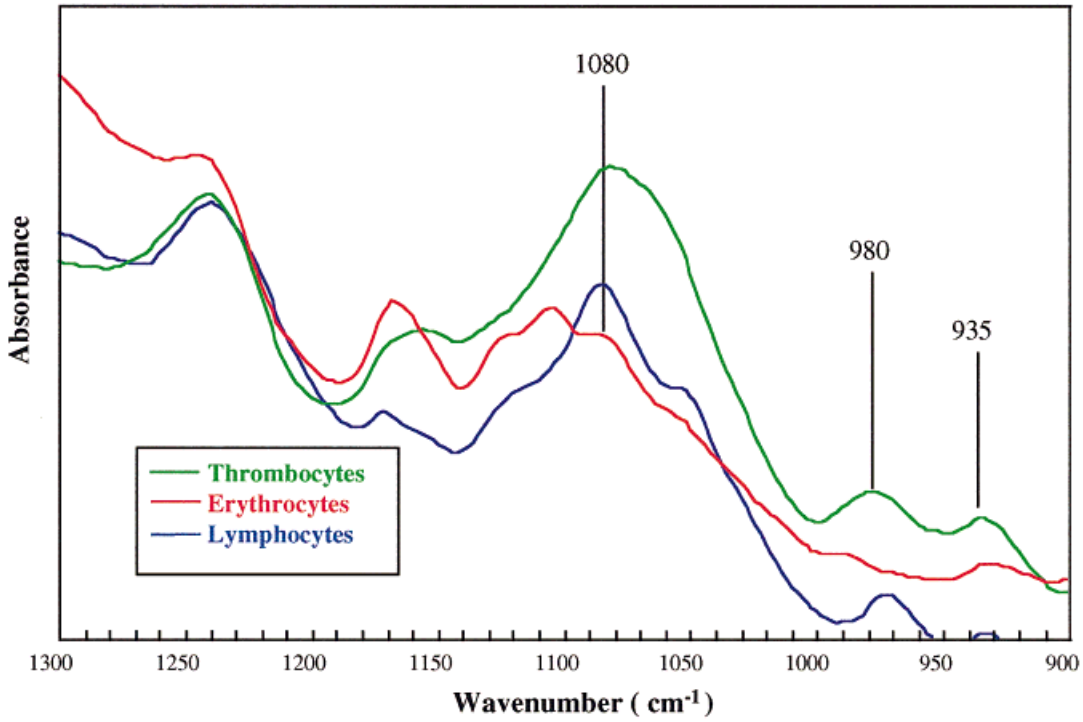

Figure 4. Averaged IR spectra of blood components (lymphocytes, thrombocytes, erythrocytes) from six volunteers in the 1300–900 cm^{-1} region.

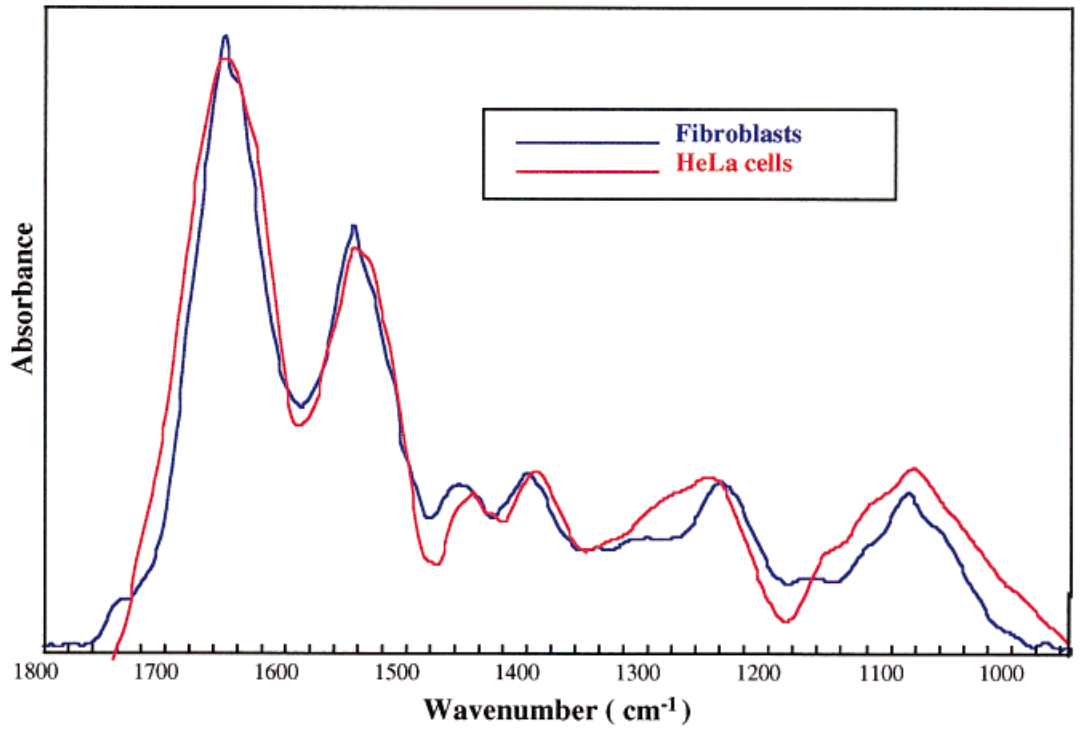

Figure 5. Average of six IR spectra of fibroblasts from one volunteer compared with the spectrum of HeLa cells.

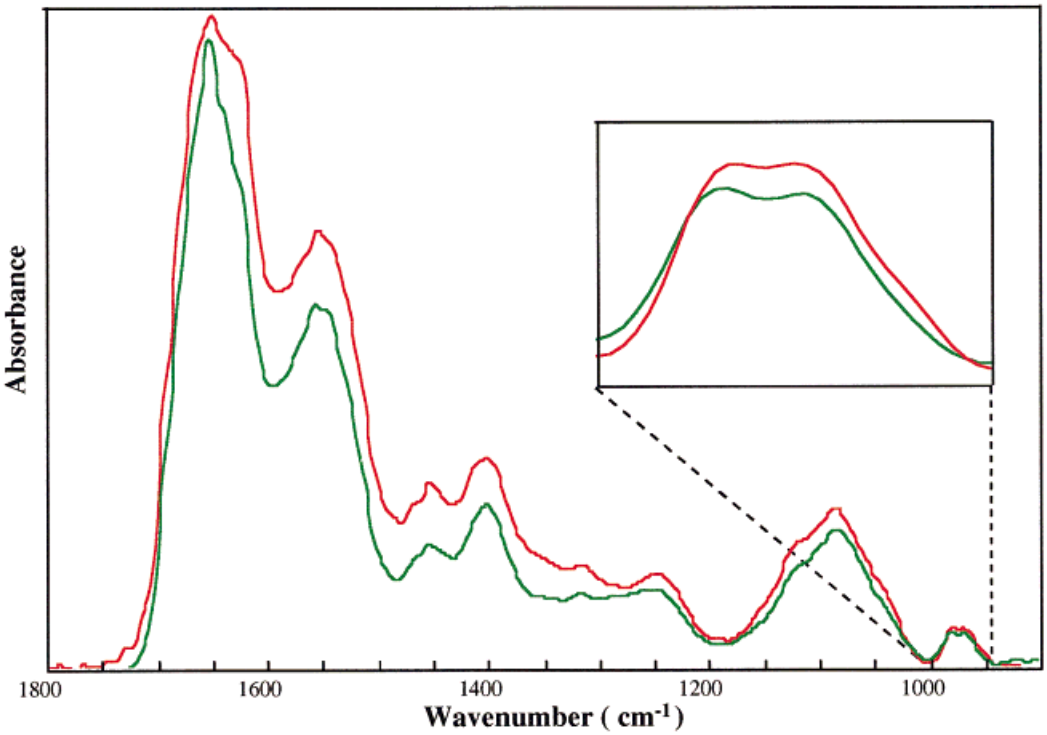

Figure 6. Spectra of semen from two individuals. The insert depicts the distinctive doublet at 981/968 cm^{-1}.

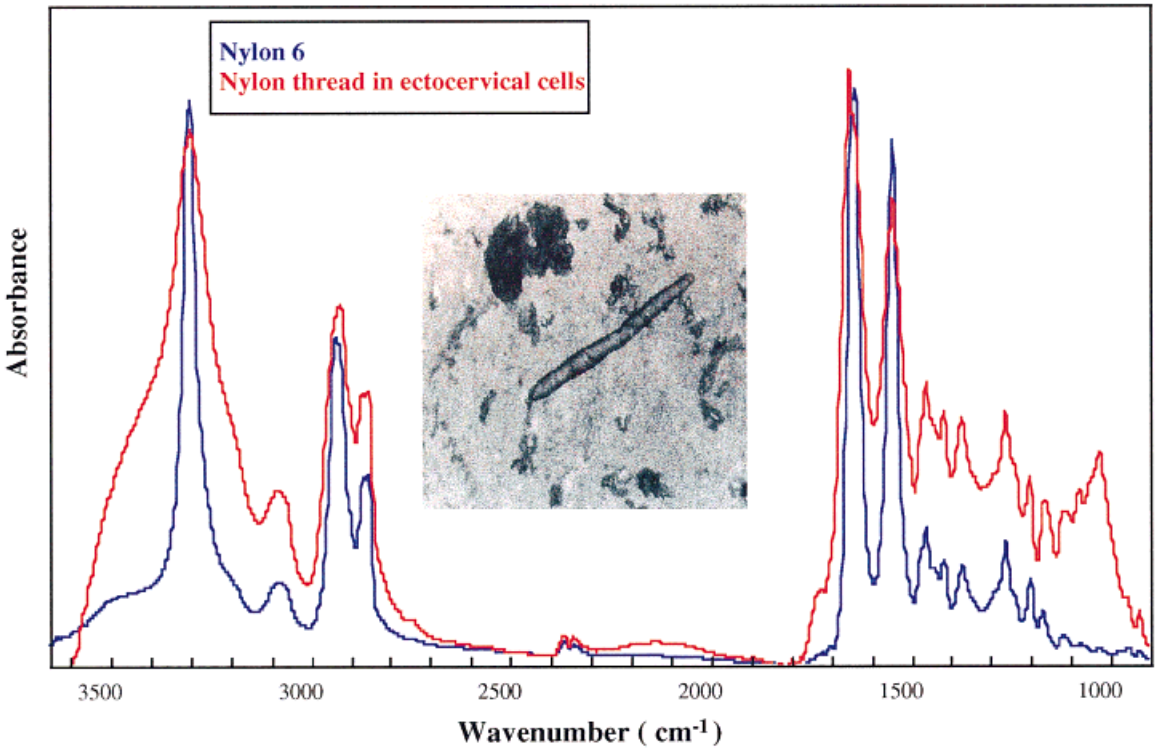

Figure 7. Photograph of a nylon thread embedded in cervical cells (120×) with the corresponding spectrum compared with a spectrum of nylon 6.

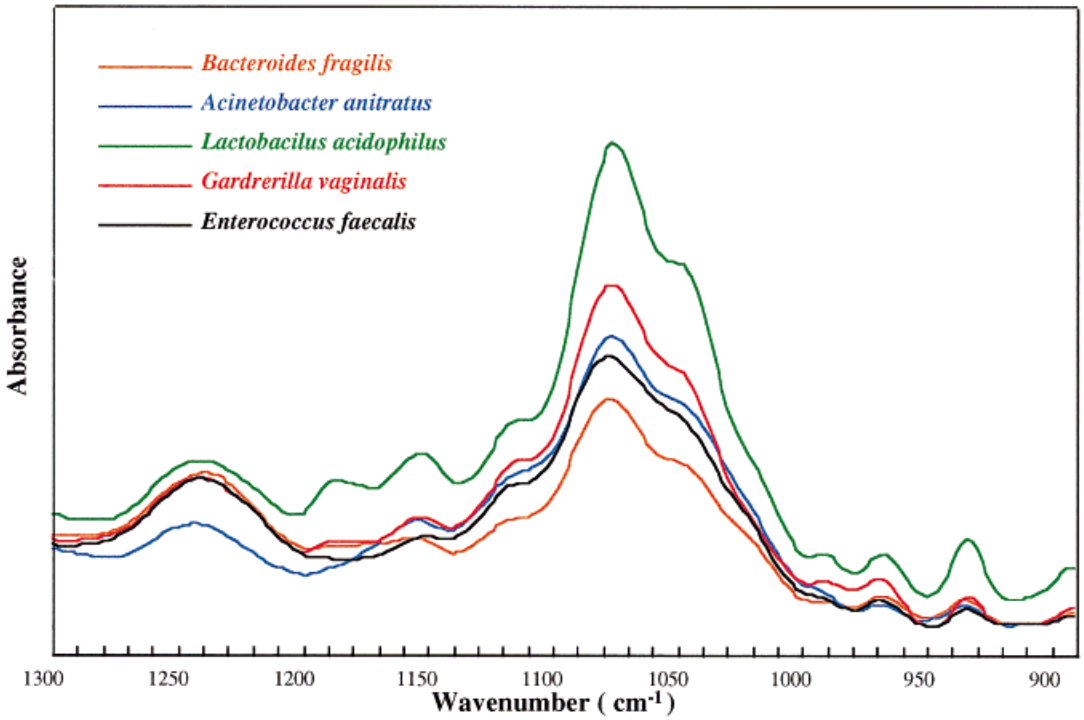

Figure 8. Averaged spectra from 5 out of the 12 bacterial species investigated showing the polysaccharide region 1150–1000 cm^{-1}.

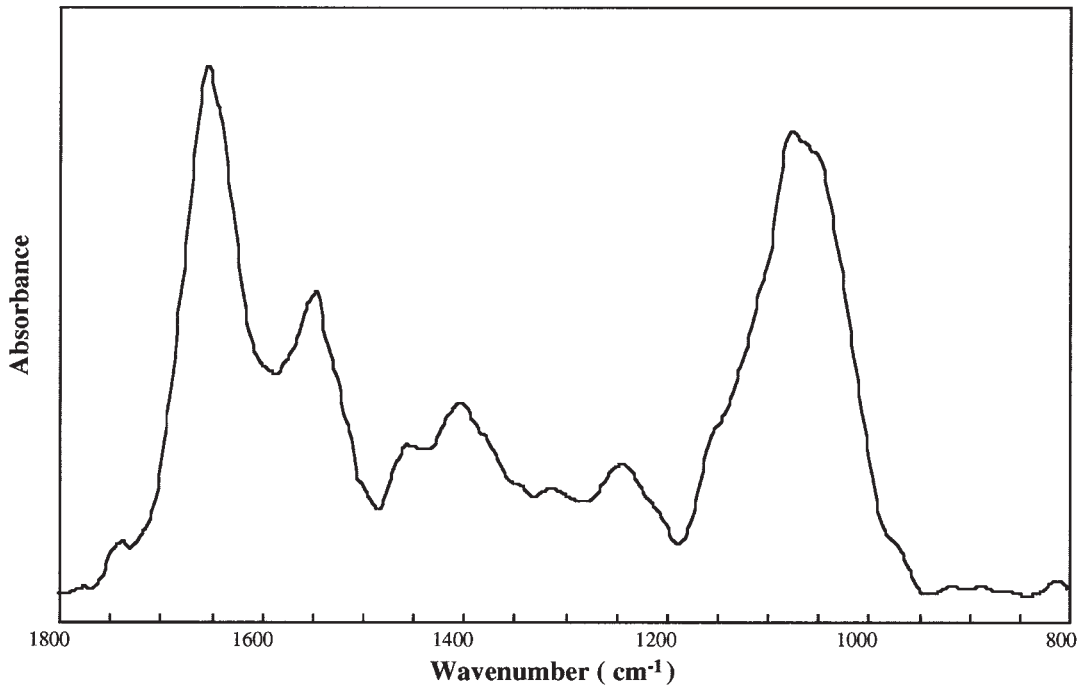

Figure 9. Spectrum of *Candida albicans* showing intense bands in the polysaccharide region (1150–900 cm^{-1}).

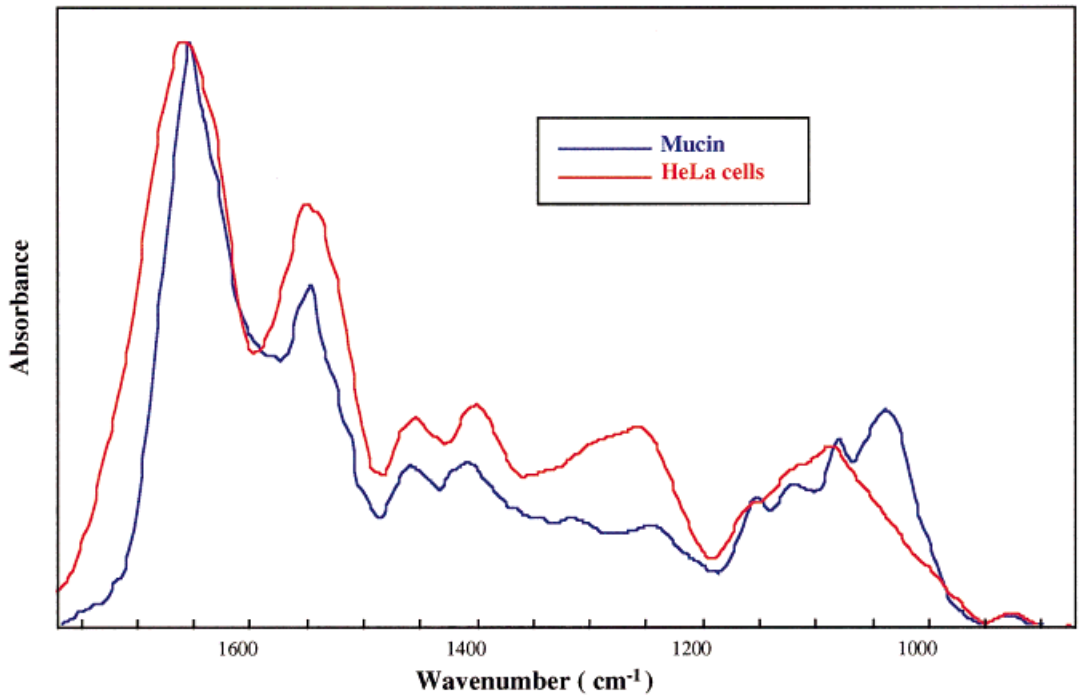

Figure 10. Spectra of endocervical mucin compared with the HeLA cell spectrum showing overlapping ν_s PO_2^- at 1080 cm^{-1}.

band appearing at ≈ 1085 cm^{-1} attributed by Nauman et al.[39] as indicative of polysaccharides. It should be noted that the bacterial cell density per sample well from the cultured strains we investigated would far exceed bacterial populations in any cervical sample, and so absorption by bacterial phosphate bands and polysaccharides would be minimal and consequently would not obscure cervical cell spectra.

Yeast

The spectrum of *Candida albicans,* shown in Figure 9, also contains bands that could potentially confound spectral diagnosis with strong and broad polysaccharide bands at 1024 cm^{-1} and 1050 cm^{-1}. However, like bacteria the contamination is usually minimal, and one would expect it to be insignificant in the vast majority of samples.

Mucins

The human endocervical mucosa consists of a system of glandular crypts lined with ciliated and nonciliated (secretory) columnar cells.[40] The surface and glandular epithelium of the cervix contains abundant mucin,[41] hence cervical mucins are a potential confounding variable. Figure 10 depicts a spectrum of mucin taken during the secretory phase of the menstrual cycle and a spectrum of HeLa cells. The spectrum of mucin exhibits a reduction in glycogen band intensity at 1024 cm^{-1} and a pronounced ν_s PO_2^- band at 1084 cm^{-1}, which is of very similar intensity to the corresponding band in the HeLa cell spectra. The bands at 1050 and 1150 cm^{-1} in the mucin sample are those usually attributed to C—O stretches and are of similar intensity to the corresponding bands in the HeLa spectrum. Consequently, visual inspection of the phosphodiester/polysaccharide region could lead to an erroneous diagnosis if this region is the only region considered for diagnostic purposes. It should be noted that both the quantity and types of mucins vary over the menstrual cycle[42] and a more detailed investigation into cervical mucins is required before the clinical application of FTIR technology.

CONCLUSION

An investigation into the potential confounding variables associated with cervical Pap smears

indicates that extreme care must be taken if visual inspection of the spectra or simple comparison of the relative intensities of a few bands are the only diagnostic indicators. The use of ethanol as a preparative, fixative, and dehydrating agent has some advantages over saline including the retention of glycogen within the cells. Leukocytes and especially lymphocytes, which proliferate and locally accumulate as a result of tissue damage or an underlying pathology, can obscure the phosphodiester/carbohydrate region (1300–1000 cm^{-1}). If examination of the phosphodiester/carbohydrate region is the only diagnostic indicator a variation in the numbers of endocervical cells in the sample could also confound spectroscopic diagnosis. Other factors that could potentially result in spectral misdiagnosis include the following: (1) severe infestations of *C. albicans* may occur, although such infestations only occur in a small percentage of smears; (2) spectra of fibroblasts closely resemble spectra of malignantly transformed cells which may provide a diagnostic indicator for severe invasive carcinoma and carcinoma *in situ;* (3) endocervical mucins also obscure the phosphodiester/carbohydrate region and closely resemble malignant epithelial cells; (4) sperm contamination could also lead to an erroneous assessment, although sperm has a number of characteristic bands enabling unique spectral identification; (5) thrombocytes exhibit strong bands in the phosphodiester/carbohydrate region; however, they can be discerned by characteristic bands below 1000 cm^{-1}. Spectra of common bacteria associated with the female genital tract generally exhibit strong polysaccharide bands in the 1300–1000 cm^{-1} region. However, severe contamination of the transformation zone with bacteria would only occur in a small percentage of smears. Given the number of potential confounding variables associated with cervical histology, a multivariate statistical analysis or neural network discrimination of the infrared spectra is the most promising approach and we are currently investigating both these methods of analysis.

This work was partially supported by grants from the Royal Women's Hospital and the Australian Research Council. The authors also acknowledge the contributions from Victorian Cytology Service for analysis of cervical samples; the Cytogenetics Department at the Royal Women's Hospital; Dr. Brian Cooke for advice on thrombocyte preparation; Toni Gartside, Leanne Hannah, and Rita Rawson for preparation and culture of microorganisms; and Gillian Paterson, Paul Kyle, and William Dandie for advice on leukocyte preparation.

REFERENCES

1. C. E. Mountford, E. J. Delikatny, M. Dyne, K. T. Holmes, W. B. Mackinnon, R. Ford, J. C. Hunter, I. D. Truskett, and P. Russell, "Uterine cervical punch biopsies can be analysed by ^{1}H MRS," *Magnetic Resonance in Medicine,* **13,** 324–331 (1990).
2. C. E. Mountford, L. C. Wright, K. T. Holmes, W. B. Mackinnon, P. Gregory, and R. M. Fox, "High-resolution proton nuclear magnetic resonance analysis of metastatic cancer cells," *Science,* **226,** 1415–1417 (1984).
3. K. T. Holmes and C. E. Mountford, "Identification of triglyceride in malignant cells," *Magnetic Resonance in Medicine,* **93,** 407–409 (1991).
4. C. E. Mountford, W. B. Mackinnon, P. Russell, A. Rutter, and E. J. Delikatny, "Human cancers detected by proton MRS and chemical shift imaging ex vivo," *Anticancer Res.,* **16**(3B): 1521–1531 (1996).
5. R. R. Alfano, G. C. Tang, A. Pradhan, W. Lam, D. S. J. Choy, and E. Opher, "Fluorescence spectra from cancerous and normal human breast tissue," *IEEE J. Quantum Electron.,* **23,** No. 10 (1987).
6. L. V. Uspenskii, M. I. Kuzin, and I. A. Ablitsov, "Laser fluorescence spectroscopy in intraoperative diagnosis and staging of lung cancer," *Khirungiia,* **3,** 31–33 (1996).
7. A. Leunig, K. Rick, H. Steep, et al., "Fluorescence imaging and spectroscopy of 5-aminolevulinic acid induced protoporphyrin IX for the detection of neoplastic lesions in the oral cavity," *Amer. J. Surg.,* **172**(6), 674–677 (1996).
8. M. Jackson and H. H. Mantsch, "IR spectroscopy: An insight into diseased tissue," *Analysis,* Oct./Nov. S10–S15 (1995).
9. H. H. Mantsch and M. Jackson, "Molecular spectroscopy in biodiagnostics (from Hippocrates to Herschel and beyond)," *J. Mol. Struct.,* **347,** 187–206 (1995).
10. H. Fabian, M. Jackson, L. Murphy, P. H. Watson, I. Fichtner, and H. H. Mantsch, "A comparative infrared spectroscopic study of human breast tumors and breast tumor cell xenografts," *Biospectroscopy,* **1,** 37–45 (1995).
11. R. Manoharan, Y. Wang, and M. S. Feld, "Histio-

chemical analysis of biological tissues using Raman spectroscopy," *Spectrochim. Acta, Part A,* **52,** 215–249 (1996).

12. C. J. Frank, D. C. B. Redd, T. S. Gansler, and R. L. McCreery, "Characterization of human breast biopsy specimens with near-IR Raman spectroscopy," *Anal. Chem.,* **66,** 319–326 (1994).
13. P. T. T. Wong, R. K. Wong, T. A. Caputo, T. A. Godwin, and B. Rigas, "Infrared spectroscopy of exfoliated human cervical cells: Evidence of extensive structural changes during carcinogenesis," *Proc. Natl. Acad. Sci. U.S.A.,* **88,** 10988–10992 (1992).
14. P. T. T. Wong, R. K. Wong, and M. F. K. Fung, "Pressure-tuning FT-IR study of human cervical tissues," *Appl. Spectrosc.,* **47,** 1058–1062 (1993).
15. Z. Ge, C. W. Brown, and H. J. Kisner, "Screening Pap smears with near-infrared spectroscopy," *Appl. Spectrosc.,* **49,** 432–436 (1995).
16. B. R. Wood, M. A. Quinn, F. R. Burden, and D. McNaughton, "An investigation into FTIR spectroscopy as a diagnostic tool for cervical cancer," *Biospectroscopy,* **2**(3), 154–164 (1996).
17. B. J. Morris, C. Lee, B. N. Nightingale, et al. "Fourier transform infrared spectroscopy of dysplastic, papillomavirus-positive cervicovaginal lavage specimens," *Gynecologic Oncology,* **56**(2), 245–249 (1995).
18. P. T. T. Wong, S. Lacelle, M. F. K. Fung, M. Senterman, N. Z. Mikhael, "Characterization of exfoliated cells and tissues from human endocervix and ectocervix by FTIR and ATR/FTIR spectroscopy," *Biospectroscopy,* **1**(5), 357–364 (1995).
19. H. M. Yadzi, M. A. Bertrand, and P. T. T. Wong, "Detecting structural changes at the molecular level with Fourier transform infrared spectroscopy—A potential tool for prescreening preinvasive lesions of the cervix," *Acta Cytologica,* **40**(4), 664–668 (1996).
20. T. D. Brock and M. T. Madigan, *The Biology of Microorganisms,* 6th ed., Prentice-Hall International Inc., UK, 1991.
21. H. A. Taimir-Riahi and T. Agbebavi, "Carbohydrates interaction with monovalent ions," *Carbohydr. Res.,* **241,** 25–35 (1993).
22. M. V. Fraile and P. Carmona, "Structural study of human very low density lipoproteins by infrared spectroscopy," *Spectrochim. Acta, Part A,* **51,** 551–563 (1996).
23. M. Jackson, L.-P. Choo, P. H. Watson, W. C. Halliday, and H. H. Mantsch, "Beware of connective tissue proteins: Assignment implications of collagen absorptions in infrared spectra of human tissues," *Biochim. Biophys. Acta,* **1270,** 1–6 (1995).
24. P. T. T. Wong, E. D. Papavassiliou, and B. Rigas, "Phosphodiester stretching bands in the infrared spectra of human tissues and cultured cells," *Appl. Spectrosc.,* **45,** 1563–1567 (1991).
25. M. Fung Kee Fung, K. Senterman, N. Z. Mikael, S. Lacelle, and P. T. T. Wong, "Pressure-tuning Fourier transform infrared spectroscopic study of carcinogenisis in human endometrium," *Biospectroscopy,* **2**(3), 155–165 (1996).
26. P. T. T. Wong, M. Cadrin, and S. W. French, "Distinct infrared spectral features in liver tumor tissue of mice: Evidence of structural modifications at the molecular level," *Exp. Mol. Pathology,* **55,** 269–284 (1991).
27. B. Rigas, S. Morgello, I. S. Goldman, and P. T. T. Wong, "Human colorectal cancers display abnormal Fourier transform infrared spectra," *Proc. Natl. Acad. Sci. U.S.A.,* **87,** 8140–8144 (1990).
28. J. M. Legal, M. Manfait, and T. Theophanides, "Applications of FTIR spectroscopy in structural studies of cells and bacteria," *J. Mol. Struct.,* **242,** 397–407 (1991).
29. F. S. Parker, *Applications of Infrared Spectroscopy in Biochemistry, Biology, and Medicine,* Plenum Press, New York, 1971.
30. J. M. Sanchez-Ruiz and M. Martinez-Carrion, "A Fourier-transform infrared spectroscopic study of the phosphoserine residues in hen egg phosvitin and oval bumin," *Biochemistry,* **27,** 3338–3342 (1988).
31. W. Zeroual, M. Manfait, and C. Choisy, "FT-IR spectroscopy study of perturbations induced by anti-biotic on bacteria," *Pathologie Biologie,* **43**(4), 300–304 (1995).
32. (a) D. Hopwood, "Fixation and Fixatives," pp. 23–46; (b) H. C. Cook, "Carbohydrates" pp. 173–214 in, *Theory and Practice of Histological Techniques,* 4th ed., ed. by J. D. Brancroft and A. Stevens, Churchill Livingstone, Edinburgh, 1996.
33. D. W. Fawcett and W. Bloom, *Bloom and Fawcett A Textbook of Histology,* 11th ed., W. B. Saunders Company, Philadelphia, 1986.
34. D. P. Stites, A. I. Terr, and T. G. Parslow, *Basic & Clinical Immunology,* 8th ed., Prentice-Hall International Inc., Englewood Cliffs, NJ, 1994.
35. A. J. Vander, J. H. Sherman, and D. S. Luciano, *Human Physiology—The Mechanisms of Body Function,* 2nd ed., McGraw-Hill, New York, 1975.
36. D. Nauman, V. Fijala, H. Labischinski, and P. Giesbrecht, "The rapid differentiation and identification of pathogenic bacteria using Fourier transform infrared spectroscopic and multivariate analysis," *J. Mol. Struct.,* **174,** 165–170 (1988).
37. D. Helm, H. Labischinski, G. Schallehn, and D. Nauman, "Classification and identification of bacteria by Fourier-transform infrared spectroscopy," *J. Gen. Microbiol.,* **137,** 69–79 (1991).
38. D. Helm, H. Labischinski, and D. Nauman, "Elaboration of a procedure for identification of bacteria

using Fourier-transform IR spectral libraries: A stepwise correlation approach," *J. of Microbiol. Meth.,* **14,** 127–142 (1991).
39. D. Nauman, H. Labischinski, and D. Helm, "Microbiological characterizations by FTIR spectroscopy," *Nature,* **351**(6321), 81–82 (1991).
40. E. S. E. Hafez, "Structural and ultrastructural parameters of the uterine cervix," *Obstet. Gynecol. Surv.,* **37,** 507–516 (1982).
41. W. B. Atkinson, L. B. Shettlers, and E. T. Engels, "A histochemical analysis of the cervix uteri," *Am. J. Obstet. Gynecol.,* **56,** 712–716 (1948).
42. E. A. Wakefield and M. Wells, "Histochemical study of endocervical glycoproteins throughout the normal menstrual cycle and adjacent to cervical intraepithelial neoplasia," *Int. J. Gynecol. Pathol.,* **4**(3), 230–239 (1985).